Journal of the Optical Society of America B
OPTICAL PHYSICS

Instrumentation limitation on a polarization-based entangled photon source

YASEERA ISMAIL,[1,*] STUTI JOSHI,[1] ANDREW FORBES,[2] AND FRANCESCO PETRUCCIONE[1,3]

[1]University of KwaZulu-Natal, School of Chemistry and Physics, Private Bag X54001, Durban 4000, South Africa
[2]University of Witwatersrand, School of Physics, Johannesburg, South Africa
[3]National Institute for Theoretical Physics, Durban, South Africa
*Corresponding author: Ismaily@ukzn.ac.za

Received 6 January 2017; revised 13 March 2017; accepted 11 April 2017; posted 11 April 2017 (Doc. ID 284166); published 5 May 2017

Free-space optical communication is hindered by turbulence resulting in spatial modal dispersion of the optical beam. Here we mimic in the laboratory the far-field turbulence effects on entangled photons in the polarization basis. We make use of a diffractive optical element to simulate turbulence distortions and measure the entanglement as a function of the turbulence strength. We show that the standard method of coincidence detection using single-mode-fiber coupling to single-photon counters results in spatial mode dependence of entanglement even though it is not measured with spatial modes. We find that the overall coupling inefficiency of the detected coincidence caused by spatial mode dispersion in free space can be corrected by the use of a multimode fiber. Our results suggest that care is required in the choice of a detection system for free-space quantum communication systems.

OCIS codes: (060.2605) Free-space optical communication; (260.5430) Polarization; (050.1970) Diffractive optics; (060.2310) Fiber optics; (010.1330) Atmospheric turbulence.

https://doi.org/10.1364/JOSAB.34.001084

1. INTRODUCTION

Quantum key distribution (QKD) is an eminent application of quantum information science and is based on the notion of ensuring the security of information by a physical process of transferring information from point to point by means of quantum carriers or, more precisely, single photons [1–3]. QKD hence provides a future-proof technology for secure communications and is applicable to situations that require confidential information to remain secure for extended periods of time. Entanglement offers an extra layer of security to the key distribution process since the state of the entangled photon remains indefinite, that is, until an observation is performed [4].

Free-space quantum communication is a mooted emerging technology and as such the propagation of entangled photons through the atmosphere has become topical of late [5]. It is realized through encoding of single photons in either the spatial or polarization degree of freedom. The latter presents a formidable choice of encoding in free-space since it is robust against atmospheric perturbation. For this reason, polarization encoded QKD schemes have been extensively exploited for free-space quantum communication [5–8].

Although atmospheric perturbation is negligible in terms of change of polarization, it does affect the spatial mode of the optical beam [9]. Incidentally, the detection scheme for single-photon sources depends on the spatial mode dispersion and coupling of free-space to fiber during the process of coincidence counting. The spatial mode dispersion created by atmospheric perturbation may lead to inefficiencies in the detection scheme. These inefficiencies can manifest itself in the coupling process.

From an optical perspective, the theory of turbulence in air is based on the differences in the refractive index amid points in the atmosphere. A simplified problem of a nonviscous and isotropic atmosphere was considered by Kolmogorov [10,11], which led to a well-defined distribution for the randomness in the refractive index of the atmosphere. The significant outcome of this theory has been that the turbulence strength can be described by a distinct parameter known as the atmospheric structure constant, C_n^2. This can be implemented in the laboratory and provides a good approximation for a real atmosphere [12,13]. The atmospheric structure constant can be computed by numerical methods as well as by experimentally simulating turbulence by means of liquid crystal technology [14–18].

One of the suitable methods for generating entangled photon fields is through spontaneous parametric downconversion (SPDC) [19]. These photons are entangled in position, momentum, polarization and spatial modes, utilizing a spatially coherent pump beam. Turbulence is known to destroy the entanglement with spatial modes; here are summarized the problems and findings. In the case of spatial modes, the decay of entanglement for the evolution of a qubit pair in turbulence

has been studied both theoretically [20–25] and experimentally [26–29]. Applying entangled photons created through spatial modes to a free-space quantum channel results in the spatial modes being affected by the atmospheric turbulence [27,30], reducing the probability of detecting photons [21,31,32]. Furthermore, the imposed scattering among spatial modes [33,34] leads to a loss of entanglement in the final state measured in a specified subspace [28,35].

To overcome the effects of turbulence, as well as the necessity for a shared reference frame, hybrid orbital angular momentum (OAM) and polarization qubit states have been suggested as possible carriers providing a more robust means of communication. The aforementioned hybrid states are rotation-invariant and have been exploited to demonstrate alignment-free, robust quantum communication where qubits are encoded in the two degrees of freedom that are entangled [36–39]. Thus far, channels with two-dimensional quantum states have been demonstrated over 144 km, between the Tenerife and La Palma Island, using polarization for the encoding [5].This has also been achieved with hybrid OAM and polarization states over a distance of 210 m in a controlled environment to minimize turbulence [38] and lately over 3 km across Vienna [40].

It is thought that turbulence has no effect on polarization since the affect spatial pattern is traced out by the detector. Here we show the effects that a simulated turbulence medium has on a polarization-based entangled single-photon source specifically focusing on the detection scheme. We generate quantum states through SPDC by utilizing a concatenated type-I nonlinear crystal. The simulated turbulence medium is achieved by utilizing a diffractive plate encoded with Kolmogorov turbulence characterized by the Strehl ratio. Emphasis is placed on the detection scheme of an entangled source under turbulent conditions. Here we observe the nonclassical behavior of an entangled photon source in the presence of a simulated turbulent medium by testing the visibility of the system and verifying the Clauser–Horne–Shimony–Holt (CHSH) inequality. We perform concurrence measurements on the system to determine the entanglement of formation [41]. We focus on the detection method of single-mode-fiber (SMF) coupling of single photons stressing on the role played by the turbulence effects in the overall detection efficiency of the system.

2. THEORETICAL BACKGROUND

The effect of atmospheric turbulence on the coincidence counts of the two-photon fields for a generic situation is studied. The signal and idler photons are produced by SPDC and are detected in coincidence by fiber couplers as shown in Fig. 1(a). The detection probability of coincidence, $C(x_1, x_2)$, of a signal photon at x_1 and an idler photon at x_2 is given as [42]

$$C(x_1, x_2) = \langle \psi | \hat{E}_s^+(x_1) \hat{E}_i^+(x_2) \hat{E}_i^-(x_2) \hat{E}_s^-(x_1) | \psi \rangle, \quad (1)$$

where $\hat{E}_s^+$ and $\hat{E}_i^+$ are the positive electric field operators for the signal and idler, respectively; $\hat{E}_s^-$ and $\hat{E}_i^-$ are the negative electric field for the signal and idler, respectively; and ψ is the wave function of the two-photon field. In general, the field $\hat{E}_\alpha^+$ is the positive electric field part at position x_j and $\hat{E}_\alpha^-$ is its Hermitian adjoint. The positive electric field component after propagation through an arbitrary optical system is given as [42]

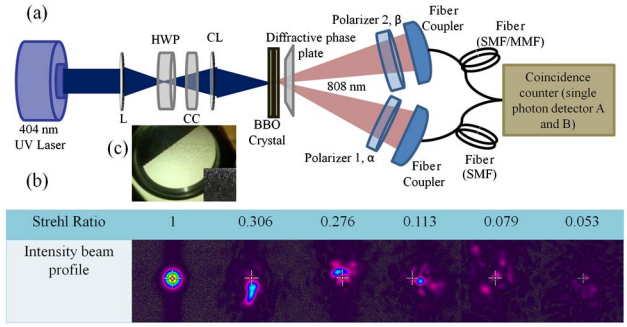

Fig. 1. Experimental setup of the entangled photon source (a) comprising a pump laser lasing at 404 nm, a lens (L), a half-wave plate (HWP), a crystal compensator (CC), a cylindrical lens (CL), two type-I concatenated BBO crystals, and a polarizer in each arm followed by a fiber coupler connected to a coincidence counter comprising single-photon avalanche detectors A and B via a SMF and a MMF. Panel (b) shows the intensity profiles of the mode dispersion for various turbulence strengths ranging from weak turbulence (Strehl ratio 0.306) to strong turbulence (Strehl ratio 0.053). The diffractive phase plate encoded with varying turbulence strength is shown in panel (c).

$$\hat{E}_\alpha^+(x, t) = \int \mathrm{d}q_\alpha H_\alpha(x, q_\alpha) \exp(-i\omega_\alpha t) \hat{b}_\alpha^-, \quad \alpha = s, i, \quad (2)$$

where $H_\alpha(x, q_\alpha)$ is the response of the signal (idler system).

The quantum state of downconverted light is defined as [42]

$$|\psi\rangle = \iint \mathrm{d}q_s \mathrm{d}q_i \Gamma(q_s, q_i) \hat{b}_s^\dagger(q_s) \hat{b}_i^\dagger(q_i) |0, 0\rangle, \quad (3)$$

where $\hat{b}_s^\dagger$ and $\hat{b}_i^\dagger$ are, respectively, the creation operators for the signal (s) and idler (i) with the transverse coordinates q_s and q_i. The vacuum state is denoted by $|0, 0\rangle$; $\Gamma(q_s, q_i)$ describes the phase matching and perfect energy conservation in the SPDC process:

$$\Gamma(q_s, q_i) = \int \mathrm{d}q_p U(q_p) \delta(q_p - q_s - q_i) \tilde{\varsigma}(q_s, q_i), \quad (4)$$

where

$$\tilde{\varsigma}(q_s, q_i) = \mathrm{sinc}\left(\frac{\Delta q L}{2}\right) \exp\left(-i\frac{\Delta q L}{2}\right); \quad (5)$$

L is the crystal length; $\Delta q = |q_s - q_i|^2 / 2k_p$ for $k_s \approx k_i \approx k_p/2$, where k_s, k_i and k_p are the signal, idler and pump beam wavenumber, respectively; and $U(q_p)$ defines the field of the pump beam.

Substituting Eqs. (2)–(5) into Eq. (1) and considering the two-photon field is propagated through a turbulent atmosphere, we have

$$\begin{aligned} C(x_1, x_2) = & \frac{4\pi k_p}{L\sqrt{\gamma^2 + 1}} \iint \iint \left\langle U_p\left(-\frac{x_1' + x_2'}{2}\right) \right. \\ & \times \left. U_p^*\left(-\frac{x_1'' + x_2''}{2}\right) \right\rangle \\ & \times \exp\left[-\frac{(x_1' + x_2')^2 k_p}{4L(\gamma + i)} - \frac{(x_1'' + x_2'')^2 k_p}{4L(\gamma - i)}\right] \\ & \times \langle h_s(x_1, x_1') h_s^*(x_1, x_1'') h_i(x_2, x_2') h_i^*(x_2, x_2'') \rangle \\ & \times \mathrm{d}x_1' \mathrm{d}x_1'' \mathrm{d}x_1' \mathrm{d}x_2'', \end{aligned} \quad (6)$$

where $\gamma = 0.455$ if $\Delta q < 0$ and $h_\alpha(x, x')$ is the inverse Fourier transform of $H_\alpha(x, q_\alpha)$, given as [43]

$$h_\alpha(x, x') = \left(-i\frac{k_\alpha}{2\pi z}\right)^{1/2} \exp\left[i\frac{k_\alpha}{2z}(x - x')^2 + \phi_\alpha(x, x')\right], \quad \alpha = s, i, \tag{7}$$

where z is the longitudinal coordinate. For a Gaussian pump beam, we have [44]

$$\langle U(x_1')U^*(x_2')\rangle = A \exp\left[-\frac{x_1'^2 + x_2'^2}{\sigma^2}\right], \tag{8}$$

where A is a positive constant and σ is the beam waist.

Since in our experiment we used a diffractive plate encoded with Kolmogorov turbulence to study the turbulence effect, the phase turbulence $\phi_\alpha(x, x')$ for a Kolmogorov model is defined as [45]

$$\langle \exp[\phi_\alpha^*(x_1, x_1') + \phi_\alpha(x_2, x_2')]\rangle = \exp\left[-\frac{(x_1 - x_2)^2 + (x_1 - x_2)(x_1' - x_2') + (x_1' - x_2')^2}{\rho_\alpha^2}\right], \tag{9}$$

where $\rho_\alpha = (0.55C_n^2k_\alpha^2z)^{-3/5}$ $(\alpha = s, i)$.

The turbulence level is described by C_n^2. This can be further defined in terms of the Strehl ratio, which is the measure of optical deformation of the field and can be expressed as [46]

$$S = \frac{I}{I_0} = \exp(\mu^2), \tag{10}$$

where I is the optical intensity of the aberrated field, I_0 is the optical intensity of the un-aberrated field and μ^2 is the phase error function, which can be expressed in terms of ρ_α as

$$\mu^2 = 1.03\left(\frac{D}{\rho_\alpha}\right)^{5/3}, \tag{11}$$

where D is the thickness of the diffractive plate. Within the paraxial approximations, we have assumed that $\Delta_q = |q_s - q_i|^2/2k_p$ for $k_s \approx k_i \approx k_p/2$ as per Eq. (5).

A theoretical plot of the detection scheme ranging from weak to strong turbulence using Eq. (6) is illustrated in Fig. 2. The initial parameters are as follows: the wavelength of the pump beam is assumed to be 404 nm and the crystal length is $L = 0.7$ mm. At the position of detection $(x_1 = x_2 = 0)$, the coincidence counts drop as the turbulent strength is increased, which is defined in terms of the Strehl ratio.

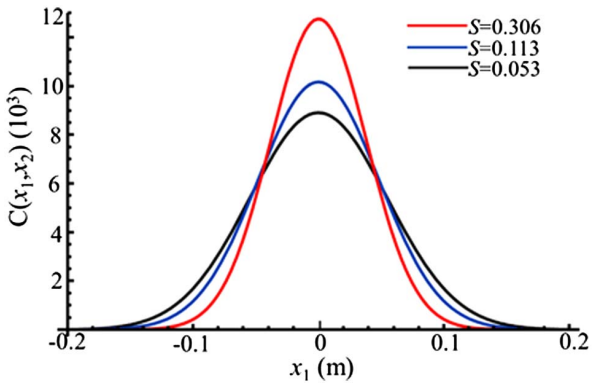

Fig. 2. Theoretical description of the detection scheme in terms of coincidence for various turbulence levels ranging from weak turbulence (0.306) to strong turbulence (0.053).

3. EXPERIMENTAL SETUP AND RESULTS

The generic scheme for an entanglement-based free-space QKD link is centered upon a photon source emitting single photons in pairs through the atmosphere toward a legitimate party. The experimental setup illustrated in Fig. 1(a) depicts the conditions imposed on entangled photon pairs associated with a free-space link; the turbulent plate was mounted such that both photons of the source passed through the turbulent medium.

Entangled photon pairs were generated at a wavelength of 808 nm produced by two type-I beta barium borate (BBO) crystals concatenated with the active axis perpendicular to each other [47]. The nonlinear crystals were illuminated with a 404 nm laser beam from a continuous-wave diode laser operating at 20 mW. In conjunction, a half-wave plate was used to set the polarization of the pump beam orientation to be diagonal relative to both BBO axes, allowing an equal probability of horizontally and vertically polarized photons being generated in accordance with the state

$$|\psi\rangle = \frac{1}{\sqrt{2}}[|V\rangle_s|V\rangle_i + e^{i\phi}|H\rangle_s|H\rangle_i], \tag{12}$$

where $|V\rangle$ and $|H\rangle$ are the vertical and horizontal states, respectively, and s and i denote the signal and idler, respectively.

A polarizer was placed in each of the free arms for measurement purposes. The photon pairs were collected using a free space-to-fiber coupler containing a collecting lens of focal length $f = 11$ mm. SMFs and multimode fibers (MMFs) were used to guide the light from the fiber coupler to single-photon avalanche detectors, which were connected to a coincidence counter where the photon pairs were registered. The verification of entanglement lies in the determination of the visibility of the system, depicting the polarization correlation of photon pairs, and the violation of the CHSH inequality [48].

The atmospheric turbulence was simulated using a diffractive phase plate encoded with Kolmogorov turbulence. The phase plate is fabricated for varying turbulence within a 5 by 5 grid ranging in turbulence strength (weak to strong). The closeness of pixels within this grid indicated the variation in the turbulence as shown in Fig. 1(c). The strength of the plate was quantified based on the Strehl ratio, which is the measure of the quality of optical deformation [48]. This was determined by the ratio of the intensity of the beam after and before the turbulent plate. For a case of zero turbulence, the Strehl ratio is said to be 1; this value decreases as the turbulence strength increases [48].

The aforementioned analysis was performed by constructing a simple system comprising a 632 nm He–Ne laser, a Fourier lens and an imaging system. The Fourier lens was placed a focal length away from the turbulent plate, which was imaged with a Spiricon Beamgage CCD camera placed a focal length (100 mm) away from the Fourier lens (far field). Measurements of intensity profiles for each row of the plate were carried out 10 times from which the Strehl ratio was determined.

Prior to incorporating the turbulent plate into the entanglement source, the propagation of the optical beam was studied. During this propagation, the Gaussian beam underwent various turbulent strengths, as it traversed across the plate, as shown in Fig. 1(b), resulting in a Strehl ratio as defined in Eq. (10), ranging from 0.306 (least turbulent) to 0.053 (most turbulent). We proceed by considering the effects that the spatial modal dispersion caused by the turbulence has on the entangled photons as illustrated in Fig. 3. Experimentally, we observe the coincidence counts for an integration time of 5 s. It was observed that a decrease in Strehl ratio resulted in a decrease in coincidence counts, which was depicted theoretically and confirmed experimentally.

For the measurement of the nonclassical behavior of the source, and for the purpose of practicality, both photons were allowed to propagate through the simulated turbulent medium. This mimics the situation where a pair of entangled photons is generated and sent to two different entities, namely, Alice and Bob as in the case of a key distribution process.

Focus was placed on understanding the spatial mode dependence on the standard detection method based on using SMF coupling in an entangled photon source by comparing the results obtained using a detection method with interchanging fibers (single- and multi-mode). This allowed the observation of the coincidence dependence due to the influence of turbulence.

The overall efficiency of the system is limited by the coupling efficiency, which is due to the fiber mode selection, namely, single- or multi-mode. A SMF is limited to the propagation of single-mode TEM_{00} only whereby all other modes are annihilated within the fiber. The other contributing factor, which influences the coupling efficiency, although less significant than mode selection, is the acceptance angle of the coupling area.

Previous numerical studies of SMFs within a turbulent medium have shown that an increase in turbulence strength results in a decrease in the intensity detected [49,50]. A MMF offers an increase in efficiency since it accepts all modes, not only modes of the order of TEM_{00}.

The visibility of the generated photon pairs in the polarization bases is shown in Fig. 4, where both detection methods were compared. One of the challenges faced when replacing the single-mode coupling fibers was the saturation of the detectors, which was overcome by replacing only one of the SMFs in the scheme presented in Fig. 1(a). We found that, for the standard detection method using a SMF, the measured visibility dropped 10% as the turbulent strength was increased to its strongest region (red and blue columns for the rectilinear and diagonal bases, respectively). This was expected as observed experimentally and theoretically in Fig. 3 for both SMF and MMF; an increase in turbulence results in a decrease in coincidence counts. Interchanging the SMF with a MMF resulted in an improved detection efficiency (purple and green columns for the rectilinear and diagonal bases, respectively), and, hence, a more stable visibility detection.

Similarly, this was observed for the violation of the CHSH inequality. In Fig. 5, we show the verification of the CHSH inequality for both detection methods (SMF and MMF) as the turbulence strength increases. The general trend is similar to that observed for the visibility. There was an improvement in the CHSH inequality measurements using a combination of a SMF and a MMF. For the various Strehl ratios, the CHSH inequality measured was centered on 2.695 ± 0.05 as observed in Fig. 5. The MMF has a larger core radius than a SMF and accepts all modes, TEM_{nm}.

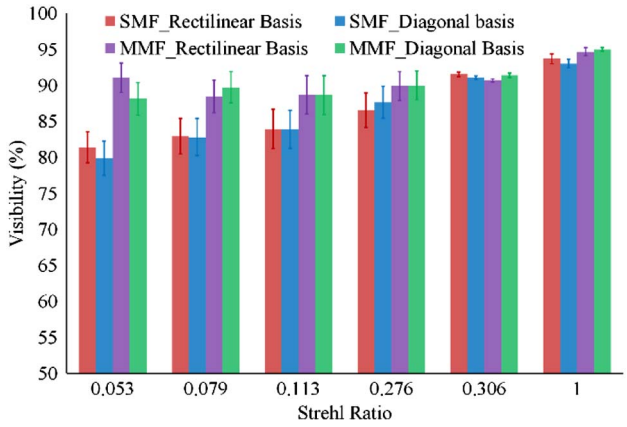

Fig. 4. Visibility of entanglement for various Strehl ratios using a SMF and a MMF detection scheme for rectilinear and diagonal bases. The detection schemes presented use a SMF and a MMF.

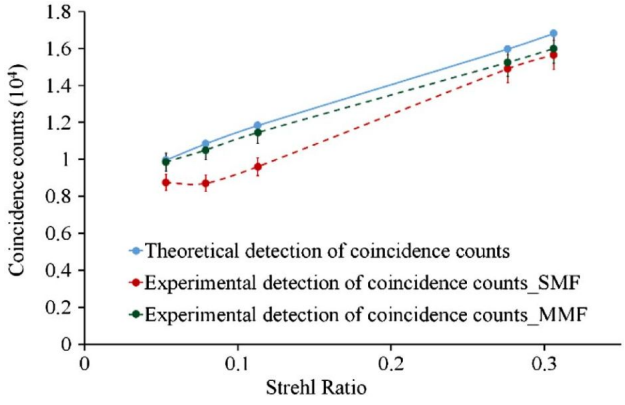

Fig. 3. Theoretical and experimental detection of coincidence counts using a SMF and a MMF fiber when both detectors are at positions $x_1 = x_2 = 0$.

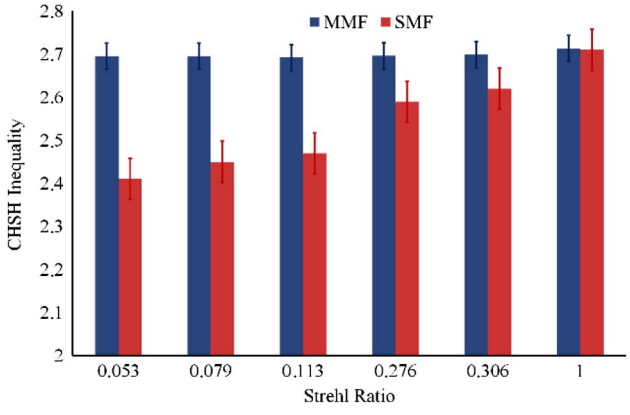

Fig. 5. Violation of CHSH inequality for various Strehl ratios using a SMF and a MMF detection scheme. The detection schemes presented use a SMF and a MMF.

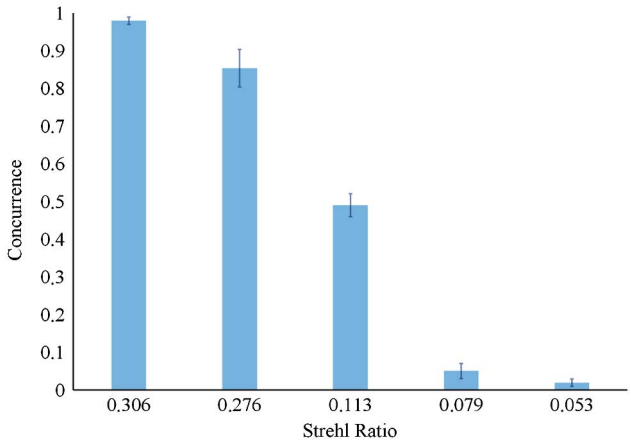

Fig. 6. Measurement of the decay of entanglement for various Strehl ratios using a SMF detection scheme.

Concurrence is a good measure of entanglement as it is computable and does not change under local operations and classical communication, and gives rise to the entanglement of formation for pure and mixed states. Maximally entangled states or, more specifically, Bell states give rise to a concurrence of 1, which decays toward 0 as the states becomes separable. The method of concurrence was applied to the photon pairs for each of the different turbulent strengths based on the implementation of state tomography. The concurrence measured for the various turbulent strengths, illustrated in Fig. 1(rows 1 to 5 ranging in Strehl ratio from 0.306 to 0.053), is shown in Fig. 6. The detection scheme utilized was that for a SMF. For a Strehl ratio of 0.306 (row 1), the observed concurrence is less than the ideal case of 1. As the turbulent strength increases, there is a noticeable decrease in the measured concurrence. This indicates a loss of security within a QKD scheme. This could be improved with the use of a MMF.

4. CONCLUSION

We studied the effects that a simulated turbulent medium has on an entangled photon source. We showed that the standard detection method results in a spatial mode dependence on the coincidences, even if the detection is not measured with spatial modes. We found that the overall coupling inefficiency of the detected coincidence caused by spatial mode dependence can be corrected using a detection method coupled with a MMF.

These results suggest that it is imperative to design a system taking into consideration all the constraints of the environment when considering free-space communication specifically to QKD whereby the quantum channel is influenced by turbulence especially if spatial mode dispersion is a significant effect imposed on the system.

Acknowledgment. This work is based on research supported by the South African Research Chair Initiative of the Department of Science and Technology and National Research Foundation as well as the Council for Scientific and Industrial Research, National Laser Centre. The authors would like to extend a thank you to Prof. Mark Tame for his feedback during the editing process.

REFERENCES

1. N. Gisin, G. Ribordy, W. Tittel, and H. Zbinden, "Quantum cryptography," Rev. Mod. Phys. **74**, 145–195 (2002).
2. S. Wiesner, "Conjugate coding," SIGACT News **15**(1), 78–88 (1983).
3. C. H. Bennett and G. Brassard, "Quantum cryptography: public key distribution and coin tossing," in *IEEE International Conference on Computers, Systems and Signal Processing*(1984), pp. 175–179.
4. A. K. Ekert, "Quantum cryptography based on Bell's theorem," Phys. Rev. Lett. **67**, 661–663 (1991).
5. R. Ursin, F. Tuefenbacher, T. Schmitt-Manderbach, H. Weier, T. Scheidl, M. Lindethal, B. Blauensteiner, T. Jennewein, J. Perdigues, P. Trojek, B. Ömer, M. Fürst, M. Meyenburg, J. Rarity, Z. Sodnik, C. Barbieri, H. Weinfurter, and A. Zeillinger, "Entanglement-based quantum communication over 144 km," Nat. Photonics **3**, 481–486 (2007).
6. X.-S. Ma, T. Herbst, T. Scheidl, D. Wang, S. Kropatschek, W. Naylor, B. Wittmann, A. Mech, J. Kofler, E. Anisimova, V. Makarov, T. Jennewein, R. Ursin, and A. Zeillinger, "Quantum teleportation over 143 kilometers using active feed-forward," Nature **489**, 269–273 (2002).
7. J. Yin, J. G. Ren, H. Lu, Y. Cao, H. L. Yong, Y. P. Wu, C. Liu, S. K. Liao, F. Zhou, Y. Jiang, X. D. Cai, P. Xu, G. S. Pan, J. J. Jia, Y. M. Huang, H. Yin, J. Y. Wang, Y. A. Chen, C. Z. Peng, and J. W. Pan, "Quantum teleportation and entanglement distribution over 100 kilometer free-space channels," Nature **488**, 185–188 (2012).
8. T. Herbst, T. Scheidl, and M. Fink, "Teleportation of entanglement over 143 km," Proc. Natl. Acad. Sci. **112**, 14202–14205 (2015).
9. X. Zhu and J. M. Khan, "Free-space optical communication through atmospheric turbulence channels," IEEE Trans. Commun. **50**, 1293–1300 (2002).
10. A. N. Kolmogorov, "The local structure of turbulence in incompressible viscous fluid for very large Reynolds numbers," Dokl. Akad. Nauk SSSR **30**, 301–305 (1941).
11. A. N. Kolmogorov, "Dissipation of energy in the locally isotropic turbulence," Dokl. Akad. Nauk SSSR **32**, 16–18 (1941).
12. D. L. Fried, "Statistics of geometrics representation of wavefront distortion," J. Opt. Soc. Am. **55**, 1427–1431 (1965).
13. D. L. Fried, "Diffusion analysis for the propagation of mutual coherence," J. Opt. Soc. Am. **58**, 961–969 (1968).
14. G. D. Love and J. Gourlay, "Intensity-only modulation for atmospheric scintillation correction by liquid-crystal spatial light modulators," Opt. Lett. **21**, 1496–1498 (1996).
15. G. D. Love, "Wavefront correction and production of Zernike modes with a liquid crystal spatial light modulator," Appl. Opt. **36**, 1517–1524 (1997).
16. G. T. Bold, T. H. Barnes, J. Gourlay, R. R. Sharples, and T. G. Haskell, "Practical issues for the use of spatial light modulators in adaptive optics," Opt. Commun. **148**, 323–330 (1998).
17. D. C. Dayton, S. L. Browne, S. P. Sandven, J. D. Gondlewski, and A. V. Kudryashov, "Theory and laboratory demonstrations on the use of a nematic liquid crystal phase modulator for controlled turbulence generation and adaptive optics," Appl. Opt. **37**, 5579–5589 (1998).
18. L. Burger, I. A. Litvin, and A. Forbes, "Simulating atmospheric turbulence using a phase-only spatial light modulator," S. Afr. J. Sci. **104**, 129–134 (2008).
19. D. C. Burnham and D. L. Weinberg, "Observation of simultaneity in parametric production of optical photon pairs," Phys. Rev. Lett. **25**, 84–87 (1970).
20. B. J. Smith and M. G. Raymer, "Two-photon wave mechanics," Phys. Rev. A **74**, 062104 (2006).
21. C. Gopaul and R. Andrews, "The effects of atmospheric turbulence on entangled orbital angular momentum states," New J. Phys. **9**, 94 (2007).
22. A. K. Jha, G. A. Tyler, and R. W. Boyd, "Effects of atmospheric turbulence on the entanglement of spatial two-qubit states," Phys. Rev. A **81**, 053832 (2010).
23. F. S. Roux, "Infinitesimal-propagation equation for decoherence of an orbital-angular-momentum-entangled biphoton state in atmospheric turbulence," Phys. Rev. A **83**, 053822 (2011).

24. J. R. Gonzalez Alonso and T. A. Brun, "Protecting orbital-angular-momentum photons from decoherence in a turbulent atmosphere," Phys. Rev. A **88**, 022326 (2013).
25. N. D. Leonhard, V. N. Shatokhin, and A. Buchleitner, "Universal entanglement decay of photonic-orbital-angular-momentum qubit states in atmospheric turbulence," Phys. Rev. A **91**, 012346(2015).
26. B.-J. Pors, C. H. Monken, E. R. Eliel, and J. P. Woerdman, "Transport of orbital-angular-momentum entanglement through a turbulent atmosphere," Opt. Express **19**, 6671–6683 (2011).
27. M. Malik, M. O'Sullivan, B. Rodenburg, M. Mirhosseini, J. Leach, M. P. J. Lavery, M. J. Padgett, and R. W. Boyd, "Influence of atmospheric turbulence on optical communications using orbital angular momentum for encoding," Opt. Express **20**, 13195–13200 (2012).
28. A. H. Ibrahim, F. S. Roux, M. McLaren, T. Konrad, and A. Forbes, "Orbital-angular-momentum entanglement in turbulence," Phys. Rev. A **88**, 012312 (2013).
29. S. K. Goyal, A. H. Ibrahim, F. S. Roux, T. Konrad, and A. Forbes, "The effect of turbulence on entanglement-based-free-space quantum key distribution with photonics orbital angular momentum," J. Opt. **18**, 064002 (2016).
30. B. Rodenburg, M. P. J. Lavery, M. Malik, M. N. O'Sullivan, M. Mirhosseini, D. J. Robertson, M. Padgett, and R. W. Boyd, "Influence of atmospheric turbulence on states of light carrying orbital angular momentum," Opt. Lett. **37**, 3735–3737 (2012).
31. C. Paterson, "Atmospheric turbulence and orbital angular momentum of single photons for optical communication," Phys. Rev. Lett. **94**, 153901 (2005).
32. G. A. Tyler and R. W. Boyd, "Influence of atmospheric turbulence on the propagation of quantum states of light carrying orbital angular momentum," Opt. Lett. **34**, 142–144 (2009).
33. C. Chen, H. Yang, S. Tong, and Y. Lou, "Changes in orbital-angular-momentum modes of a propagated vortex Gaussian beam through weak-to-strong atmospheric turbulence," Opt. Express **24**, 6959–6975 (2016).
34. R. Neo, M. Goodwin, J. Zheng, J. Lawrence, S. Leon-Saval, J. Bland-Hawthorn, and G. Molina-Terriza, "Measurement and limitations of optical orbital angular momentum through corrected atmospheric turbulence," Opt. Express **24**, 2919–2930 (2016).
35. F. S. Roux, T. Wellens, and V. N. Shatokhin, "Entanglement evolution of twisted photons in strong atmospheric turbulence," Phys. Rev. A **92**, 012326 (2015).
36. C. Souza, C. Borges, A. Z. Khoury, J. Huguenin, L. Aolita, and S. Walborn, "Quantum key distribution without a shared reference frame," Phys. Rev. A **77**, 032345 (2008).
37. V. D'Ambrosio, E. Nagali, S. P. Walborn, L. Aolita, S. Slussarenko, L. Marrucci, and F. Sciarrino, "Complete experimental toolbox for alignment-free quantum communication," Nat. Commun. **3**, 961 (2012).
38. G. Vallone, V. D'Ambrosio, A. Sponselli, S. Slussarenko, L. Marrucci, F. Sciarrino, and P. Villoresi, "Free-space quantum key distribution by rotation-invariant twisted photons," Phys. Rev. Lett. **113**, 060503 (2014).
39. O. J. Farías, V. D'Ambrosio, C. Taballione, F. Bisesto, S. Slussarenko, L. Aolita, L. Marrucci, S. P. Walborn, and F. Sciarrino, "Resilience of hybrid optical angular momentum qubits to turbulence," Sci. Rep. **5**, 8424 (2015).
40. M. Krenn, J. Handsteiner, M. Fink, R. Fickler, and A. Zeilinger, "Twisted photon entanglement through turbulent air across Vienna," Proc. Natl. Acad. Sci. USA **112**, 14197–14201 (2015).
41. W. K. Wooters, "Entanglement of formation of an arbitrary state of two qubits," Phys. Rev. Lett. **80**, 2244–2248 (1998).
42. B. E. Saleh, A. F. Abouraddy, A. V. Sergienko, and M. C. Teich, "Duality between partial coherence and partial entanglement," Phys. Rev. A **62**, 043816 (2000).
43. X. Du, D. Zhao, and O. Korotkova, "Changes in the statistical properties of stochastic anisotropic electromagnetic beams on propagation in the turbulent atmosphere," Opt. Express **15**, 16909–16915 (2007).
44. L. Mandel and E. Wolf, *Optical Coherence and Quantum Optics* (Cambridge University, 1995).
45. H. T. Yura, "Mutual coherence function of a finite cross section optical beam propagating in a turbulent medium," Appl. Opt. **11**, 1399–1406 (1972).
46. A. Janssen, S. van Haver, P. Dirksen, and J. Braat, "Zernike representation and Strehl ratio of optical systems with numerical aperture," J. Mod. Opt. **55**, 1127–1157 (2008).
47. P. G. Kwiat, E. Waks, A. G. White, I. Appelbaum, and P. H. Eberhard, "Ultrabright source of polarization entangled photons," Phys. Rev. A **60**, R773–R776 (1999).
48. D. Dehlinger and M. W. Mitchella, "Entangled photons, nonlocality, and Bell inequalities in the undergraduate laboratory," Am. J. Phys. **70**, 903–910 (2002).
49. X. Zhao, H. Jiang, and H. Zheng, "Fibre coupling efficiency through turbulence medium for long and short," IEEE Optoelectron. Microelectron. **17**, 334–336 (2012).
50. J. Niu and J. Xu, "Coupling efficiency of laser beams to multimode fibre," Opt. Commun. **274**, 315–319 (2007).